NeuroImage 42 (2008) 1639–1653

Contents lists available at ScienceDirect

NeuroImage

journal homepage: www.elsevier.com/locate/ynimg

Intelligence and EEG phase reset: A two compartmental model of phase shift and lock

R.W. Thatcher *, D.M. North, C.J. Biver

EEG and NeuroImaging Laboratory, Applied Neuroscience Research Institute, St. Petersburg, FL, USA

ARTICLE INFO

Article history:
Received 19 February 2008
Revised 29 April 2008
Accepted 9 June 2008
Available online 18 June 2008

Keywords:
EEG phase reset
Phase shift duration
Phase lock duration
Intelligence

ABSTRACT

Objectives: The purpose of this study was to explore the relationship between EEG phase reset and performance on the Wechsler Intelligence test.
Methods: The electroencephalogram (EEG) was recorded from 19 scalp locations from 378 subjects ranging in age from 5 years to 17.6 years. The Wechsler Intelligence test (WISC-R) was administered to the same subjects on the same day but not while the EEG was recorded. Complex demodulation was used to compute instantaneous EEG phase differences between pairs of electrodes and the 1st and 2nd derivatives were used to measure phase reset by phase shift duration and phase lock duration. The dependent variable was full scale I.Q. and the independent variables were phase shift duration (SD) and phase lock duration (LD) with age as a covariate.
Results: Phase shift duration (40–90 ms) was positively related to intelligence ($P<.00001$) and the phase lock duration (100–800 ms) was negatively related to intelligence ($P<.00001$). Phase reset in short interelectrode distances (6 cm) was more highly correlated to I.Q. ($P<.0001$) than in long distances (>12 cm).
Conclusions: The duration of unstable phase dynamics and phase locking represent a bounded optimization process, for example, too long a duration of phase locking then less flexibility and too short of a phase shift then reduced neural resources. A two compartmental model of local field coupling and neuron synchrony to a preferred phase was developed to explain the findings.

Introduction

Complexity in the brain is often defined by models of information theory and stochastic processes involving a balance between differentiation and integration (Tononi et al., 1994; Buzsaki, 2006). Tononi et al. (1994) showed that highly complex neural networks were characterized by neurons that were organized into densely linked groups that were sparsely and reciprocally interconnected. Small-world models of connected systems show that reduction of long distance connections and increased connectivity of local systems is a fundamental information optimization process (Watts and Strogatz, 1998). In line with these models of complexity is the fact that the development of brain connectivity as measured by EEG coherence and phase shows a developmental balance between local neural integration and long distant differentiation similar to the standard models of complexity (Thatcher et al., 1987; 2007a; Tononi et al., 1994). Human intelligence is also directly correlated to brain complexity as measured by the EEG (Anokhin et al., 1999; Giannitrapani, 1985; Thatcher et al., 1983; 2005). For example, inverse relations between EEG coherence and I.Q. have been reported in many electrode locations and different frequency bands (Marosi et al., 1999; Martin-Loeches et al., 2001; Barry et al., 2002; Silberstein et al., 2003; 2004; Thatcher et al., 1983; 2005). These studies support a general "neural efficiency" model of intelligence involving the instantaneous allocation of neural resources in which coherence is a measure of redundancy and differentiation (Haier et al., 1992; Thatcher et al. 1983, 2005, 2007a, in press).

Studies of EEG complexity, dimensionality and intelligence have also included measures of phase delays. Thatcher et al. (1983, 2005) found significant correlations between EEG phase delays and I.Q. with complex spatial relationships. Further exploration of the relationship between performance on neuropsychological tests and EEG phase is important in order to probe the deeper relations between synchrony and phase delays and intelligence. For example, the patterns of spontaneously occurring synchronous activity involve the creation of temporary differentiated neural assemblies with oscillations and covarying phase at local, regional and large scales (Breakspear and Terry, 2002a; 2002b; Rudrauf et al., 2006; Stam and de Bruin, 2004; Varela, 1995; Varela et al.,

---

* Corresponding author. NeuroImaging Laboratory, Applied Neuroscience Research Institute, St. Petersburg, Florida 33722, USA.
E-mail address: rwthatcher@yahoo.com (R.W. Thatcher).

1053-8119/$ – see front matter © 2008 Elsevier Inc. All rights reserved.
doi:10.1016/j.neuroimage.2008.06.009

2001; Freeman and Rogers, 2002; Thatcher et al., 2007b). The dynamic balance between synchronization and desynchronization is essential for normal brain function and abnormal balance is often associated with pathological conditions such as epilepsy (Lopes da Silva and Pihn, 1995; Le Van Quyen et al., 2001b; Chavez et al., 2003; Netoff and Schiff, 2002), schizophrenia (Lee et al., 2002) and dementia (Stam et al., 2002a; 2002b).

Studies of the mechanisms of synchronization and desynchronization often involve the use of a measure referred to as phase reset (PR). For example, measures of EEG phase reset have been correlated to various frequency bands during cognitive tasks (Kahana, 2006; Kirschfeld, 2005; Tesche and Karhu, 2000), working memory (John, 1968; Rizzuto et al., 2003; Damasio, 1989; Tallon-Baudry et al., 2001), sensory–motor interactions (Vaadia et al., 1995; Roelfsema et al., 1997), hippocampal long-term potentiation (McCartney et al., 2004), brain development (Thatcher et al., in press) and consciousness (Cosmelli et al., 2004; Varela et al., 2001; John, 2002; 2005). The present study builds on these previous studies by analyzing the relationship between intelligence and the two fundamental components of phase reset: 1 — phase shift duration and, 2 — phase lock duration measured in the spontaneous resting EEG.

PR occurs in coupled nonlinear oscillators when there is a sudden shift of the phase relationship of oscillators to a new value followed by a period of phase locking or phase stability also called phase synchrony (Pikovsky et al., 2003). The term phase synchrony is synonymous with phase locking and whether one refers to phase locking or phase synchrony what is important is the fact that there is a prolonged period of phase stability following a phase shift. This is important because random phase shifts without stability exhibit "white noise" distributions (Pikovsky et al., 2003; Tass, 1997). PR is also important because it results in increased EEG amplitudes due to increased phase synchrony of synaptic generators (Cooper et al., 1965; Nunez, 1995; Lopes da Silva, 1995). There are two general and equivalent methods for studying PR: 1 — narrow band decomposition and, 2 — broad band decomposition (Rudrauf et al., 2006; Le Van Quyen et al., 2001a; Bruns, 2004). Both methods use analytic transforms such as the Fourier transform, Wavelet transform and Hilbert transform. Which method is used depends on the frequency resolution desired and the nature of the transient signals that are to be detected (Rudrauf et al., 2006; Tass, 1997; Le Van Quyen et al., 2001a; Lachaux et al., 2000; Freeman et al., 2003; 2006; Freeman and Rogers, 2002). In the present paper we used complex demodulation as an analytic signal processing method similar to Lachaux et al. (2000) and Breakspear and Williams (2004) which is mathematically the Hilbert transform (Pikovsky et al., 2003; Oppenheim and Schafer, 1975). All methods measure the temporal adjustment of pairs of signals evaluated over a successive frequency range or successive intervals of time with phase stability measured by the first derivative where phase stability is when the first derivative of phase difference approximates zero or $d\varphi_{i,j}/dt \approx 0$. In general, the magnitude of phase shift is defined as the difference between the pre-shift phase value minus the post-shift phase value and if a sudden and significant phase difference occurs followed by an extended period of phase stability then the point in time when the phase shift started is the time when the first derivative exceeded some threshold value (Rudrauf et al., 2006; Tass, 1997; Tass et al., 1998; Le Van Quyen et al., 2001a; Breakspear and Williams, 2004). This point in time marks the onset of a phase shift and phase reset. EEG phase shift offset is defined in a reverse manner and the onset and offset times define the phase shift duration.

Previous studies from this laboratory on the relationship between intelligence and absolute power, coherence, amplitude asymmetry and phase differences have shown that phase and coherence produce stronger correlations to I.Q. than does absolute power (Thatcher et al., 2005). LORETA source correlations and I.Q., although weaker than coherence and phase, indicate specific timing relationships between 3-dimensional current sources and information processing (Thatcher et al., 2007a, 2007b). A study of the relationship between EEG phase shift duration ("unstable phase dynamics") and phase lock duration ("stability") and human intelligence has not been studied to date and would extend our previous studies and advance understanding about the relationship between EEG and I.Q. Therefore, the purpose of the present study is to investigate the relationship between human EEG phase reset and neuropsychological measures of intelligence in the same subjects as studied in Thatcher et al. (2005, 2007b). The null hypotheses to be tested in this study are: 1 — there are no significant correlations between measures of EEG phase reset and intelligence; 2 — there are no differences in the EEG frequency band and the correlation to intelligence; 3 — there are no differences between the left and right hemispheres and the correlation to intelligence and, 4 — there are no differences between the frontal vs. posterior brain regions and the correlation to intelligence.

Methods

Subjects

A total of 378 subjects ranging in age from 5 to 17.58 years (males = 221) were included in this study. The subjects in the study were recruited using newspaper advertisements in rural and urban Maryland (Thatcher et al., 1987; 2003; 2007a). The inclusion/exclusion criteria were no history of neurological disorders such as epilepsy, head injuries and reported normal development and successful school performance. None of the subjects had taken medication of any kind at least 24 h before testing in this study. All of the school age children were within the normal range of intelligence as measured by the Wechsler Intelligence Test (WISC-R) and were performing at grade level in reading, spelling and arithmetic as measured by the Wide Range Achievement Test (WRAT) and none were classified as learning disabled nor were any of the school aged children in special education classes. All subjects were given an eight-item "laterality" test consisting of three tasks to determine eye dominance, two tasks to determine foot dominance, and three tasks to determine hand dominance. Scores ranged from −8 (representing strong sinistral preference or left handedness), to +8 (representing strong dextral preference or right handedness). Dextral dominant children were defined as having a laterality score of ≥2 and sinistral dominant children were defined as having a laterality score of ≤−2. Only approximately 9% of the subjects had laterality scores ≤2 and 87% of the subjects had laterality scores ≥2 and thus the majority of subjects in this study were right side dominant.

EEG recording

Power spectral analyses were performed on 58 sec to 2 min 17 sec segments of EEG recorded during resting eyes closed condition. The EEG was recorded from 19 scalp locations based on the International 10/20 system of electrode placement, using linked ears as a reference. The average reference and a Laplacian reference were not used because these reference methods involve mixing the amplitude and phase from different scalp locations resulting in phase and coherence distortions as shown by Rappelsberger (1989), Kamiński and Blinowska (1991) and Essl and Rappelsberger (1998). Eye movement electrodes were applied to monitor artifact and all EEG records were visually inspected and manually edited to remove any visible artifact. Each EEG record was plotted and visually examined and split-half reliability and test re-test reliability measures of the artifacted data were computed using the Neuroguide software program (NeuroGuide, v2.3.8). Split-half reliability tests were conducted on the edited EEG segments and only records with >90% reliability were entered into the spectral analyses. The amplifier bandwidths were nominally 1.0 to 30 Hz, the outputs being 3 db down at these frequencies. The EEG was digitized at 100 Hz and up-sampled to 128 Hz and then spectral analyzed using complex demodulation (Granger and Hatanaka, 1964; Otnes and Enochson, 1978).

EEG phase differences and phase reset metrics were computed in the delta (1–4 Hz); theta (4–8 Hz); alpha frequency band (8.0–13 Hz); alpha1 (8–10 Hz); alpha2 (10–13 Hz); beta1 (13–15 Hz); beta2 (15–18 Hz); beta3 (18–25 Hz) and hi-beta (25–30 Hz). Factors used in the multivariate analysis of variance were: 1 — Hemisphere, 2 — Direction, 3 — Interelectrode distance and 4 — Age.

Complex demodulation and joint-time-frequency-analysis

Complex demodulation was used in a joint-time-frequency-analysis (JTFA) to compute instantaneous coherence and phase differences (Granger and Hatanaka, 1964; Otnes and Enochson, 1978; Bloomfield, 2000). This method is an analytic linear shift-invariant transform that first multiplies a time series by the complex function of a sine and cosine at the center frequency of each frequency band followed by a low pass filter (6th order low pass Butterworth) which removes all but very low frequencies (shifts frequency to 0) and transforms the time series into instantaneous amplitude and phase and an "instantaneous" spectrum (Bloomfield, 2000). We place quotations around the term "instantaneous" to emphasize that, as with the Hilbert transform, there is always a trade-off between time resolution and frequency resolution. The broader the band width the higher the time resolution but the lower the frequency resolution and vice versa. Mathematically, complex demodulation is defined as an analytic transform (Z transform) that involves the multiplication of a discrete time series $\{x_t,\ t=1,\ \dots,\ n\}$ by sine $\omega_0 t$ and cos $\omega_0 t$ giving

$$x_t' = x_t \sin \omega_0 t \tag{1}$$

and

$$x_t'' = x_t \cos \omega_0 t \tag{2}$$

and then apply a low pass filter F to produce the instantaneous time series, Z'_t and Z_t'' where the sine and cosine time series are defined as:

$$Z_t' = F(x_t \sin \omega_0 t) \tag{3}$$

$$Z_t'' = F(x_t \cos \omega_0 t) \tag{4}$$

and

$$2\left[(Z_t')^2 + (Z_t'')^2\right]^{1/2} \tag{5}$$

is an estimate of the instantaneous amplitude of the frequency ω_0 at time t and

$$\tan^{-1}\frac{Z_t'}{Z_t''} \tag{6}$$

is an estimate of the instantaneous phase at time t.

The instantaneous cross-spectrum is computed when there are two time series $\{y_t,\ t=1,\ 1/4,\ n\}$ and $\{y'_t,\ t=1,\ 1/4,\ n\}$ and if F [ ] is a filter passing only frequencies near zero, then, as above $R_t^2 = F[y_t \sin\omega_0 t]^2 + F[y_t \cos\omega_0 t]^2 = |F\left[y_t e^{i\omega_0 t}\right]^2|$ is the estimate of the amplitude of frequency ω_0 at time t and $\varphi_t = \tan^{-1}\left(\frac{F[y_t \sin\omega_0 t]}{F[y_t \cos\omega_0 t]}\right)$ is an estimate of the phase of frequency ω_0 at time t and

$$F\left[y_t e^{i\omega_0 t}\right] = R_t e^{i\varphi_t}, \tag{7}$$

and likewise,

$$F\left[y_t' e^{i\omega_0 t}\right] = R_t' e^{i\varphi_t} \tag{8}$$

The instantaneous cross-spectrum is

$$V_t = F\left[y_t e^{i\omega_0 t}\right] F\left[y_t' e^{-i\omega_0 t}\right] = R_t R_t' e^{i[\varphi_t - u\ V]} \tag{9}$$

and the instantaneous coherence is

$$\frac{|V_t|}{R_t^2 R_t'^2} \equiv 1 \tag{10}$$

The instantaneous phase-difference is $\varphi_t - \varphi_t'$. That is, the instantaneous phase difference is computed by estimating the instantaneous phase for each time series separately and then taking the difference. Instantaneous phase difference is also the arctangent of the imaginary part of V_t divided by the real part (or the instantaneous quadspectrum divided by the instantaneous cospectrum) at each time point.

Phase straightening

We used the phase "straightening" method of Otnes and Enochson (1978) to remove the phase angle discontinuity, i.e., where 0 and 360 are at opposite ends while in the circular distribution 0° = 360°. This procedure involves identifying the points in time when phase jumps from +180° to −180° and then adding or subtracting 360° depending on the direction of sign change resulting in phase being a smooth function of time by removing the discontinuities due to the arctangent function. We found that absolute phase differences without phase straightening gave similar results to the straightened phase differences. This is because the vast majority of EEG phase relationships are less than ±180°. However, phase straightening is important when computing the first and second derivatives of the time series of phase differences because the discontinuity between −180° and +180° can produce artifacts. Accordingly, all of the derivatives and phase reset measures in this paper were computed after phase straightening.

Computation of the 1st and 2nd derivatives of the time series of phase differences

The first derivative of the time series of phase differences between all pair wise combinations of two channels was computed in order to detect advancements and reductions of phase differences. The Savitzky–Golay procedure was used to compute the first derivatives of the time series of instantaneous phase differences using a window length of 3 time points and the polynomial degree of 2 (Savitzky and Golay, 1964; Press et al., 1994). The units of the 1st derivative are in degrees/point which was normalized to degrees per centisecond (i.e., °/cs = °/100 ms). The second derivative was computed using a window length of 5 time points and a polynomial degree of 3 and the units are degrees per centiseconds squared (i.e., $°/cs^2 = °/100\ ms^2$).

Calculation of phase reset

The time series of 1st derivatives of the phase difference from any pair of electrodes was first rectified to the absolute value of the 1st derivative (see Fig. 2). The sign or direction of a phase shift is arbitrary since two oscillating events may “spontaneously” adjust phase with no starting point (Pikovsky et al., 2003; Tass, 2007). The onset of a phase shift was defined as a significant absolute first derivative of the time series of phase differences between two channels, i.e., $d(\varphi_t - \varphi_t')/dt > 0$, criterion bounds = 5°. Phase stability or phase locking is defined as that period of time after a phase shift where there is a stable near zero first derivative of the instantaneous phase differences or $d(j_t - j_t')/dt \approx 0$. The criteria for a significant 1st derivative is important and in the present study a threshold criteria of 5° was selected because it was >3 standard deviations where the mean phase shift ranged from 25°/cs to 45°/cs. Changing the threshold to higher values was not significant, however, eliminating the threshold resulted in greater “noise” and therefore the criteria of 5° is an adequate criteria. As pointed out by Breakspear and Williams (2004) visual inspection of the data is the best method for selecting an arbitrary threshold value and the threshold value itself is less important than keeping the threshold constant for all subjects and all conditions. Fig. 1

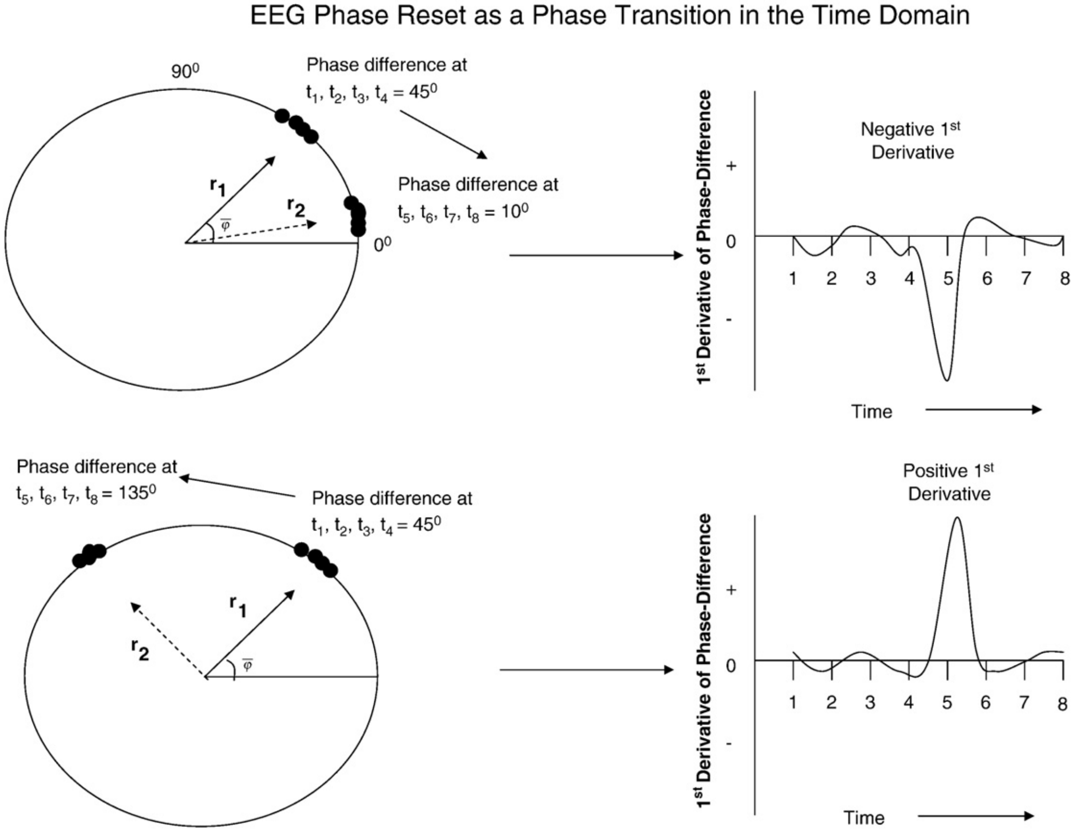

Fig. 1. Illustrations of phase reset. Left is the unit circle in which there is a clustering of phase angles and thus high coherence as measured by the length of the unit vector ***r***. The top row is an example of phase reduction and the top right is a time series of the approximated 1st derivative of the instantaneous phase differences for the time series t_1, t_2, t_3, t_4 at mean phase angle = 45° and t_5,t_6,t_7, t_8 at mean phase angle = 10°. The vector $\boldsymbol{r}_1 = 45°$ occurs first in time and the vector $\boldsymbol{r}_2 = 10°$ and 135° (see bottom left) occurs later in time. Phase reset is defined by a sudden change in phase difference followed by a period of phase locking. The onset of phase reset is between time points 4 and 5 where the 1st derivative is a maximum. The 1st derivative near zero is when there is phase locking and little change in phase difference over time. The bottom row is an example of phase advancement and the bottom right is the 1st derivative time series. The sign or direction of phase reset in a pair of EEG electrodes is arbitrary since there is no absolute “starting point” and phase shifts are often “spontaneous” and not driven by external events, i.e., self-organizing criticality. When the absolute 1st derivative ≈ 0 then two oscillating events are in phase locking and represent a stable state independent of the direction of phase shift.

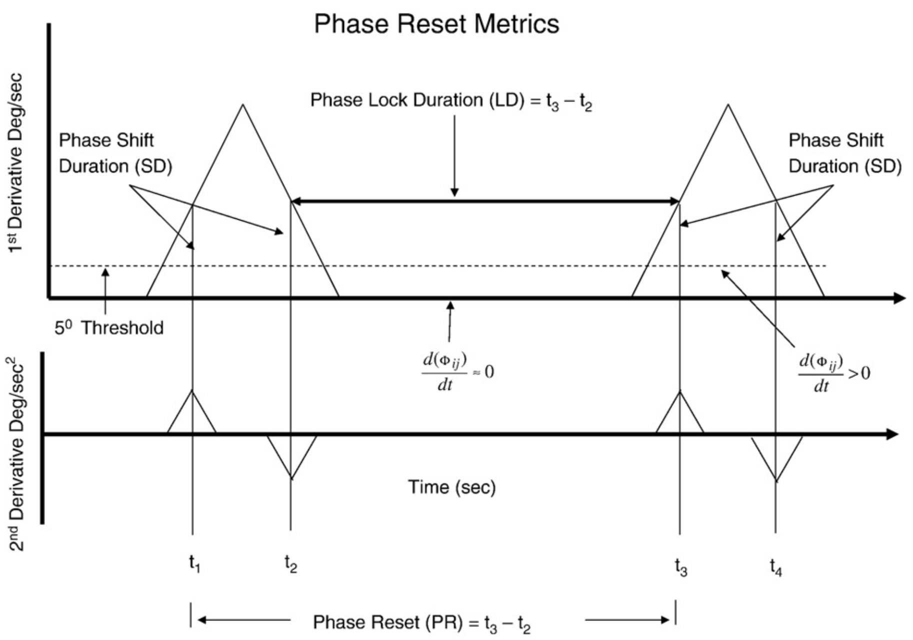

Fig. 2. Diagram of phase reset metrics. Phase shift onset was defined at the time point when a significant 1st derivative occurred (≥5°/cs) followed by a peak in the 1st derivative, phase shift duration (SD) was defined as the time from onset of the phase shift defined by the positive peak of the 2nd derivative to the offset of the phase shift defined by the negative peak of the 2nd derivative. The phase lock duration (LD) was defined as the interval of time between the onset of a phase shift and the onset of a subsequent phase shift. Phase reset (PR) is composed of two events: 1 — a phase shift and 2 — a period of locking following the phase shift where the 1st derivative ≈ 0 or PR = SD + LD. Phase locking is defined when the absolute 1st derivative of the phase difference between two oscillators approximates zero $\frac{|d(\Phi_{ij})|}{dt} \approx 0$. Phase shift onset is defined when the absolute 1st derivative of the phase difference between two oscillators is greater than zero $\frac{|d(\Phi_{ij})|}{dt} > 0$ with a threshold of ≥5°/cs.

illustrates the concept of phase reset. Phase differences over time on the unit circle are measured by the length of the unit vector ***r***. Coherence is a measure of phase consistency or phase clustering on the unit circle as measured by the length of the unit vector ***r***. The illustration in Fig. 1 shows that the resultant vector $\boldsymbol{r}_1 = \boldsymbol{r}_2$ and therefore coherence when averaged over time ≈ 1.0 even though there is a brief phase shift. As the number of phase shifts per unit time increases then coherence declines because coherence is directly related to the average amount of phase locking or phase synchrony (Bendat and Piersol, 1980).

Fig. 2 shows the time markers and definitions used in this study. As mentioned previously the peak of the absolute 1st derivative was used in the detection of the onset and offset of a phase shift and the second derivative was used to detect the inflection point which defines the full-width-half-maximum (FWHM) and phase shift duration. As seen in Fig. 2, phase reset (PR) is composed of two events: 1 — a phase shift of a finite duration (SD) and 2 — followed by an extended period of phase locking as measured by the phase lock duration (LD) and PR = SD + LD. Phase shift duration (SD) is the interval of time from the onset of phase shift to the termination of phase shift where the termination is defined by two conditions: 1 — a peak in the 1st derivative (i.e., 1st derivative changes sign from positive to zero to negative) and, 2 — a peak in the 2nd derivative or inflection on the declining side of the time series of first derivatives. The peak of the 2nd derivative marked the end of the phase shift period. Phase shift duration is the difference in time between phase shift onset and phase shift offset or $\mathrm{SD}(t) = \mathrm{S}(t)_{\mathrm{onset}} - \mathrm{S}(t)_{\mathrm{offset}}$. Phase lock duration (LD) was defined as the interval of time between the end of a significant phase shift (i.e., peak of the 2nd derivative) and the beginning of a subsequent significant phase shift, i.e., marked by the peak of the 2nd derivative and the presence of a peak in the 1st derivative or $\mathrm{LD}(t) = \mathrm{S}(t)_{\mathrm{onset}} - \mathrm{S}(t)_{\mathrm{offset}}$. In summary, two measures of phase dynamics were computed: 1 — Phase shift duration (ms) (SD) and, 2 — Phase lock duration (ms) (LD). Fig. 2 illustrates the phase reset metrics and Fig. 3 shows an example of the computation of phase reset metrics in a single subject.

Results

Multivariate regression analyses

The partial correlation coefficient was computed between each of the 171 EEG variables for phase shift duration and phase locking and full scale I.Q. scores after regressing out the covariance with age. Table 1 shows the number of statistically significant variables as well as the percentage of the total variables that were statistically significant in the seven different frequency bands for phase shift duration and for phase locking. One would expect approximately 5% of the variables to be statistically significant by chance alone or $N = 8.6$. Therefore, a Chi square test of the expected number of significant correlations by chance alone was conducted and is shown in Table 1.

The variables with statistically significant ($P < .05$) correlations were then entered into a step-wise hierarchical multivariate regression analyses in which full scale I.Q. was the dependent variable, age was the covariate and phase shift duration and phase lock duration were the independent variables. Table 2 shows the results of the multivariate analyses for correlation between full scale I.Q. and phase shift duration and phase lock duration after removing the affects of age. The multiple *R* values were statistically significant in all frequency bands for both phase shift duration and phase lock duration. Alpha1 and alpha2 frequency bands exhibited the weakest

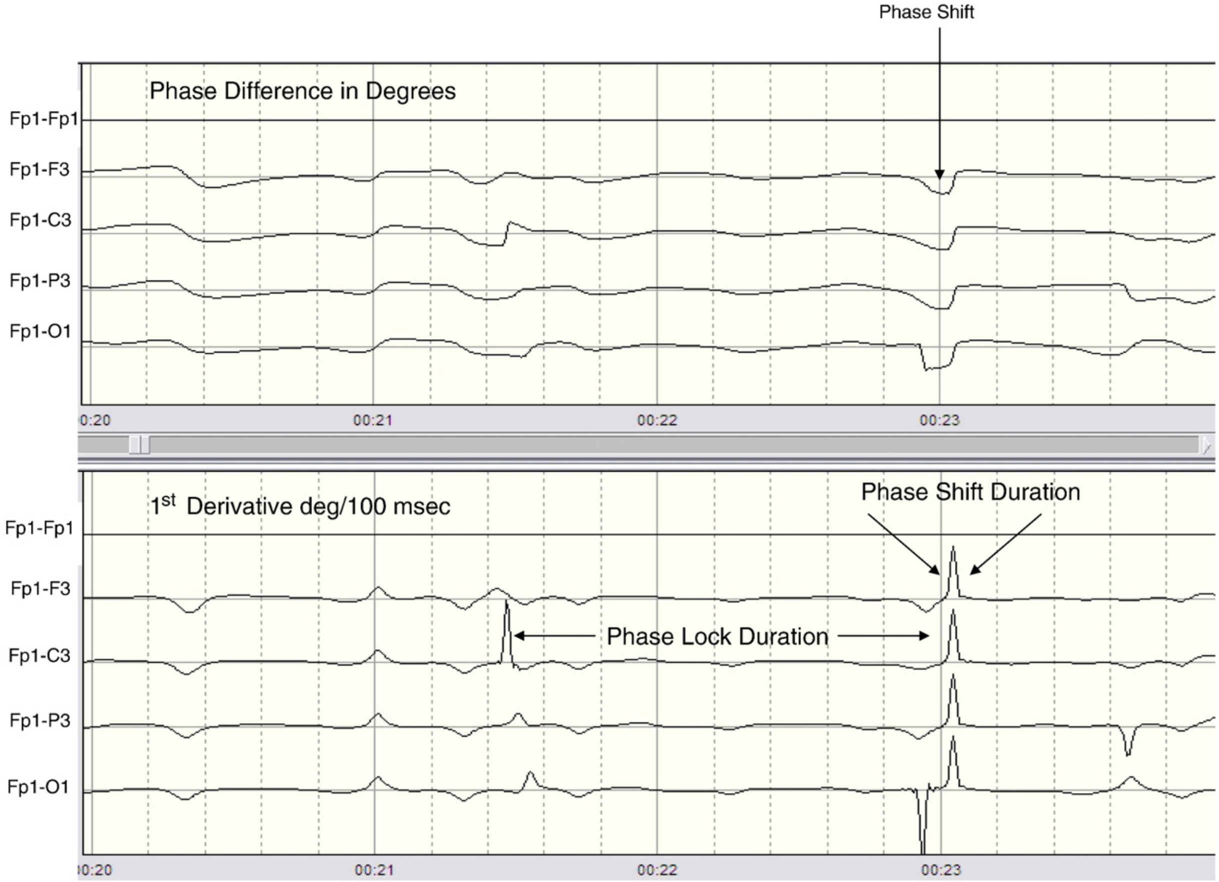

Fig. 3. Example from one subject. Top are the EEG phase differences between Fp1-F3, Fp1-C3, Fp1-P3 and Fp1-O1 in degrees. Bottom are the 1st derivatives of the phase differences in the top traces in °/cs. A 1st derivative ≥5°/cs marked the onset of a phase shift and an interval of time following the phase shift where the 1st derivative≈0 defined the phase synchrony interval as described in Fig. 2.

multiple *R* values. The overall multiple *R* when all frequencies were combined was 0.752 ($P<.0001$) for the correlation between full scale I.Q. scores and phase shift duration and 0.610 ($P<.0004$) for the correlation between full scale I.Q. and the phase lock duration. The multiple *R* when both phase shift duration and phase lock duration were entered as the dependent variables and age as the covariate was 0.826 or about 68% of the variance of full scale I.Q.

Fig. 4 shows the results of the age adjusted multivariate regression analyses for individual frequency bands and intelligence. The dependent variable was full scale I.Q., age was a covariate and the independent variables were EEG phase locking and EEG phase reset intervals in the delta, theta, alpha1, alpha2, beta1, beta2, beta3 and hi-beta frequency bands. The largest correlations were between I.Q. and theta and beta1 phase shift duration. The lowest multiple *R*s were with alpha1 and alpha2 phase lock duration.

Chi square tests of the sign of correlation

The sign of the correlation between full scale I.Q. and phase shift duration after adjusting for age was primarily positive while the sign of the correlation between I.Q. and phase lock duration was primarily negative. A Chi square test for the sign of the correlation was conducted using the null hypothesis

Table 1
The statistically significant correlations between I.Q. and PR

$N=171$	Shift duration		Lock duration	
Frequency	#	$P(X^2)$	#	$P(X^2)$
delta	34	0.0001	12	N/S
theta	18	0.0021	52	0.0001
alpha1	18	0.0021	2	N/S
alpha2	15	0.0399	1	N/S
beta1	24	0.0001	18	0.0021
beta2	15	0.0399	27	0.0001
beta3	51	0.0001	4	N/S
hi-beta	20	0.0002	13	N/S

Partial correlations and probability of X^2 using full scale IQ with phase reset adjusted for age.
Significant levelat ±.100 ($P<.05$).
Total number of electrode combinations = 171. Chi square is of the number expected at the $P<.05$ level by chance alone ($N=8.6$) vs. the observed number of statistically significant observations.

Table 2
Results of the multivariate regression analyses between WISC-R full scale I.Q. scores and EEG phase shift duration and EEG phase lock duration

Frequency	Phase shift duration			Phase lock duration		
	Multiple *R*	*P*	# of VARs	Multiple *R*	*P*	# of VARs
delta	0.293	0.0073	28	0.295	0.0001	13
theta	0.389	0.0001	16	0.322	0.0440	40
alpha1	0.290	0.0330	14	0.110	0.0001	3
alpha2	0.257	0.0001	12	0.118	0.0001	2
beta1	0.356	0.0001	20	0.335	0.0001	16
beta2	0.305	0.0001	14	0.360	0.0004	26
beta3	0.389	0.0010	42	0.216	0.0001	5
hi-beta	0.238	0.0021	17	0.241	0.0001	11
Overall	0.752	0.0001	155	0.610	0.0004	111

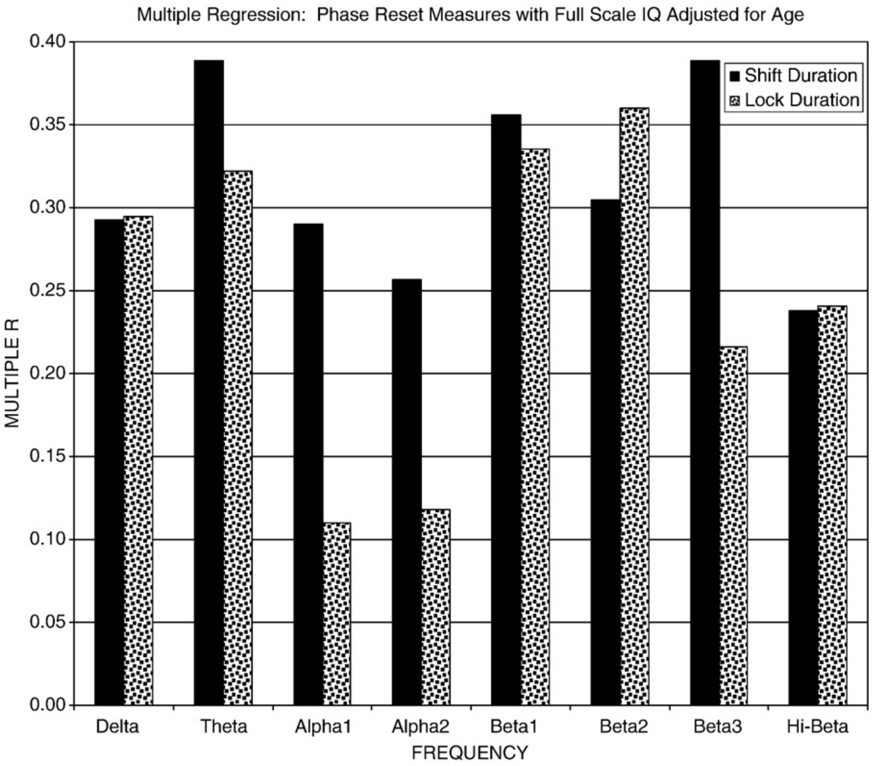

Fig. 4. Results of the multivariate regression analyses between WISC-R full scale I.Q. scores and the eight different frequency bands of EEG phase shift duration and EEG phase lock duration. The *y*-axis is the multiple *R* values and the *x*-axis is the EEG frequency bands. The black columns are phase shift duration (SD) correlations and the gray columns are the phase lock duration (LD) correlations.

expectation of 50% likelihood of a positive or negative correlation between the phase reset measures and I.Q. Table 3 shows the results of the Chi square tests for full scale I.Q. and the correlations to phase shift duration and phase lock duration. Phase shift duration was negatively correlated to full scale I.Q. while phase lock duration was positively correlated to full scale I.Q.

In order to explore the linearity and sign of the correlation between phase reset and I.Q. the subjects were sub-divided into seven full scale I.Q. groupings and then linear regression analyses were conducted using phase shift duration and phase lock duration as the independent variable and I.Q. as the dependent variable. The seven I.Q. groups were: 70 to 79 I.Q. ($N=19$); 80 to 89 I.Q. ($N=44$); 90 to 99 I.Q. ($N=67$); 100 to 109 I.Q. ($N=94$); 110 to 119 I.Q. ($N=70$); 120 to 129 I.Q. ($N=48$); 130 to 154 I.Q. ($N=31$). The results of the linear regression analyses are shown in Fig. 5. It can be seen that statistically significant linear regressions were present in which phase shift duration was positively related to full scale I.Q. and phase locking was negatively related to full scale I.Q.

Table 3
Sign Tests using Chi-square method of significant partial correlations with full I.Q. and phase reset measures of phase shift duration and phase lock duration adjusted for age

Phase reset	Shift duration				Locking duration			
Frequency	pos	neg	X^2	P	pos	neg	X^2	P
delta	34	0	34.00	0.0001	11	1	8.33	0.0001
theta	5	13	3.56	N/S	1	51	48.08	0.0001
alpha1	18	0	18.00	0.0001	2	0	N/S	N/S
alpha2	15	0	15.00	0.0001	0	1	N/S	N/S
beta1	23	1	20.17	0.0001	14	4	5.56	0.0184
beta2	14	1	11.27	0.0008	1	26	23.15	0.0001
beta3	51	0	33.11	0.0001	1	3	1.00	N/S
hi-beta	20	0	20.00	0.0001	1	12	9.31	0.0023

As seen in Fig. 5 (top), the linear regression equation for phase shift duration produced positive correlations with intercepts from approximately 78 I.Q. to 138 I.Q. points. In general, the longer the phase shift duration then the higher the full scale I.Q. A 4 ms average shift duration was related to an approximate 60 point range of I.Q. scores. The average slope of the regression equations was approximately twenty one (21) I.Q. points/ms of phase shift duration. One can equate rates of change in time to degrees of phase difference by using the peak first derivative of phase differences which were computed during the process of measuring PR (see Figs. 1–3). The mode of 1st derivatives was approximately 27°/cs or 2.7°/ms which means that the full 60 point range of I.Q. was spanned by 10.8° of phase shift.

Fig. 5 (bottom) shows the linear regression equation for phase lock duration vs. I.Q. In general, the shorter the phase lock duration then the higher the full scale I.Q. The negative correlations also exhibited intercepts from approximately 78 I.Q. to 138 I.Q. or a 60 I.Q. point range and an average phase lock duration range of approximately thirteen (13) milliseconds. This represents approximately 4.6 I.Q. points/ms of phase lock duration.

Fig. 6 are frequency histograms of phase shift duration (top) and phase lock duration (bottom) between the high I.Q. and low I.Q. groups of subjects in 6 cm distance electrode pairings. The difference in the peaks of phase shift duration for high vs. low I.Q. groups was about 3.0 ms and the difference in the peaks of phase lock duration was about 50 ms. This is a similar range of time differences in the regression analyses of the seven I.Q. groups in Fig. 5.

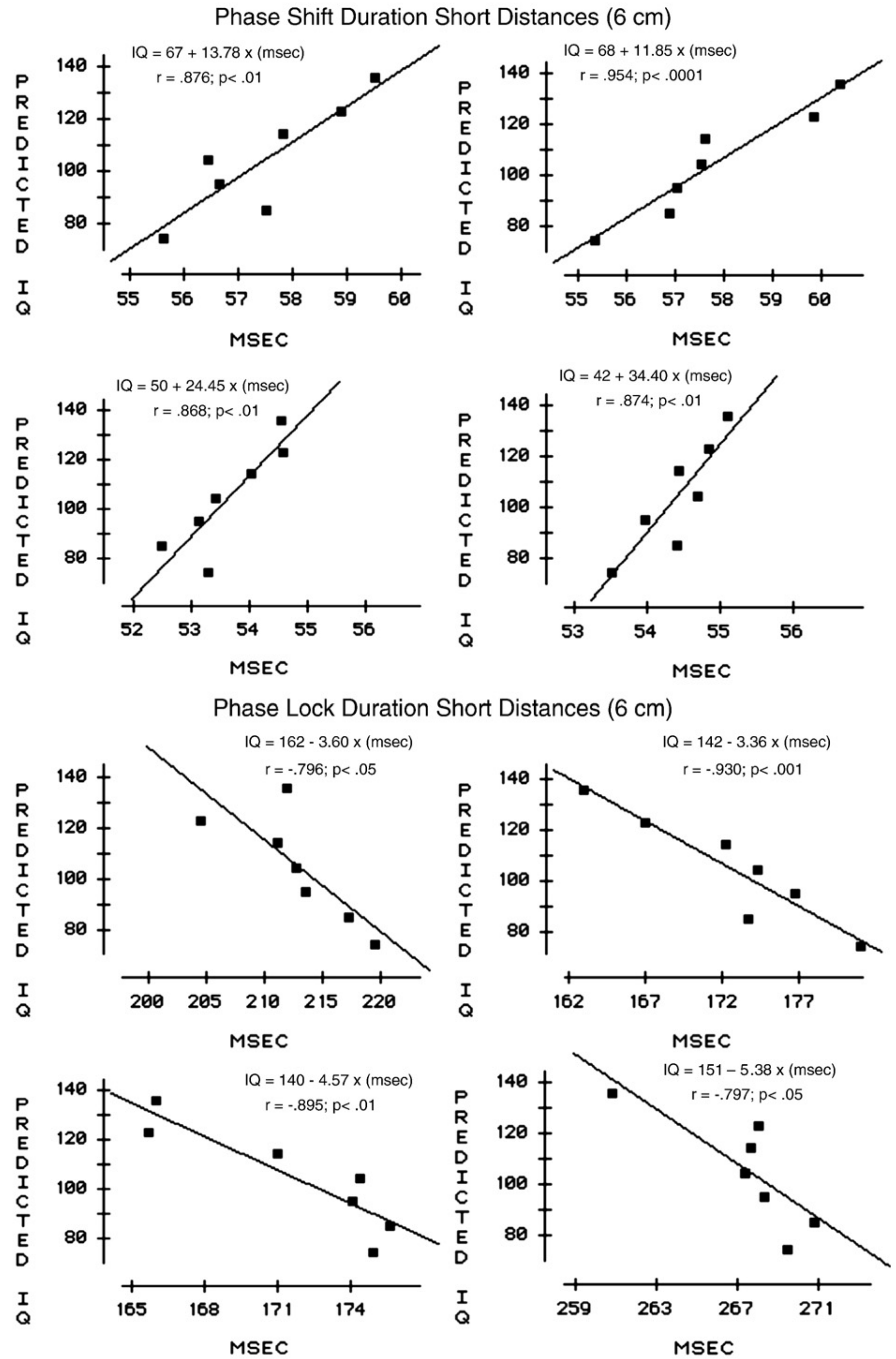

Fig. 5. Linear fit of EEG phase shift duration (top) and EEG phase lock duration (bottom) and seven full scale I.Q. groupings. The *x*-axis is EEG phase shift duration (ms) (top) and EEG phase lock duration (ms) (bottom). The *y*-axis is full scale I.Q. Examples are 6 cm interelectrode distances from P3/4-O1/2 and Fp1-F3. The correlation, *P* value and average standard deviation are shown above each regression line.

Multivariate analyses of variance phase shift duration and intelligence

Multivariate analyses of covariance (ANCOVA) were conducted for phase shift duration as the independent variable and low (I.Q.<90 to 70; $N=71$) and high full scale I.Q. (120 to 155; $N=79$) groups as the dependent variable and age as a covariate. EEG phase shift duration and phase lock duration were evaluated for direction, hemisphere, frequency and distance by limiting the analyses to five equally spaced pairs of electrodes using a multivariate analysis of variance (MANOVA) after removing the correlation with age. This reduced analysis is from the same set of electrode pairs as published by Thatcher et al. (1986, 1988, 2007a). The anterior-to-posterior direction was Fp1/2-F3/4; Fp1/2-C3/4; Fp1/2-P3/4 and Fp1/2-O1/2. The posterior-to-anterior direction was O1/2-P3/4; O1/2-C3/4; O1/2-F3/4 and O1/2-Fp1/2. The interelectrode distance was independent of direction and varied from approximately 6 cm; 12 cm; 18 cm to 24 cm for both the left and right hemisphere.

The factors for phase shift duration were left hemisphere vs. right hemisphere; direction, frequency and interelectrode

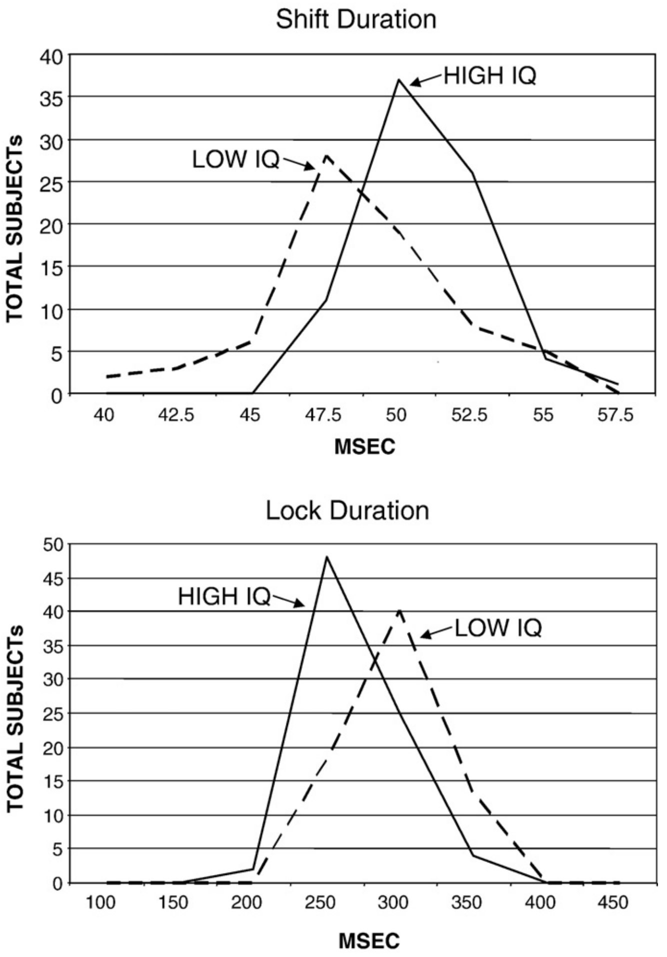

Fig. 6. Histograms of the number of subjects with phase shift durations (top) and phase lock durations (bottom) in high ($>$120 I.Q.) vs. low I.Q. ($<$90 I.Q.) groupings of subjects using 6 cm electrode pairings. *y*-axis is the number of subjects and *x*-axis is time (ms).

distance (6 cm, 12 cm, 18 cm and 24 cm). There was a statistically significant hemispheric effect with longer shift duration in the left hemisphere compared to the right ($F=7.512$, $P<0.005$) as well as a statistically significant Bonferroni post hoc test ($P<.006$). There also was a statistically significant distance effect ($F=1966$, $P<.0001$) with statistically significant Bonferroni post hoc tests ($P>.0001$) showing that the 6 cm distance exhibited a stronger effect than all other distances. There was a statistically significant direction effect ($F=305.84$, $P<.0001$) and a significant Bonferroni post hoc test ($P<.000001$) showing longer shift durations in the posterior-to-anterior direction than in the anterior-to-posterior direction. There also was a significant frequency effect ($F=7529$, $P<.0001$). Bonferroni post hoc tests showed that only beta1 vs. beta2 frequency bands were not statistically significant.

Multivariate analyses of variance phase lock duration and intelligence

Multivariate analyses of covariance (ANCOVA) were conducted for phase lock duration as the independent variable and low I.Q. (90 to 70; $N=71$) and high full scale I.Q. (120 to 155; $N=79$) groups as the dependent variable and age as a covariate. The factors for the phase lock duration were the same as for phase shift duration and were left hemisphere vs. right hemisphere; direction, frequency and interelectrode distance (6 cm, 12 cm, 18 cm and 24 cm). Unlike phase shift duration there was no statistically significant left vs. right hemisphere affect for phase locking ($F=1.82$; $P=0.1779$). Also, unlike phase shift duration there was no statistically significant effect of anterior-to-posterior vs. posterior-to-anterior directions for phase lock duration ($F=0.219$; $P=0.639$). However, there was a statistically significant distance effect ($F=1137$, $P<.0001$) with statistically significant Bonferroni post hoc tests ($P>.0001$) with 6 cm distance exhibiting a stronger effect than all other distances for both phase locking and phase shift duration. There also was a significant frequency effect ($F=6996$; $P<.0001$). Bonferroni post hoc tests were statistically significant ($P<.001$) for all frequency band comparisons.

Analyses of interelectrode distance effects and direction

Table 4 shows the correlations between full scale I.Q. and phase shift duration using the seven mean full scale I.Q. groups as in Fig. 6. It can be seen that most of the statistically significant correlations were in the 6 cm interelectrode distance and in the posterior-to-anterior direction.

Table 5 shows the correlations between full scale I.Q. and the phase lock duration using the seven mean full scale I.Q. groups as in Fig. 6. Similar to phase shift duration most of the statistically significant correlations were in the 6 cm interelectrode distance and in the posterior-to-anterior direction. The subset of anterior-to-posterior and posterior-to-anterior electrodes is described in Thatcher et al. (1986, 1998, 2007a).

Fig. 7 summarizes the number of statistically significant correlations between full scale I.Q. and phase shift duration and the phase lock duration using the seven mean I.Q. groups as in Fig. 5. It can be seen that most of the statistically significant correlations were in the local or short distance (6 cm) interelectrode distances with the next largest number at 12 cm interelectrode distances and the least number of statistically significant correlations at long interelectrode distances (18 cm and 24 cm).

Discussion

The three primary findings of this study are: 1 — there is a direct relationship between phase shift duration and an inverse relationship between phase lock duration and intelligence, 2 — shorter phase lock duration in the theta frequency band and longer phase shift duration in the beta frequency bands were most strongly related to intelligence and, 3 — the highest correlations were in short distance (6 cm) interelectrode combinations. There were no significant hemispheric differences in the correlation of phase lock duration and full scale I.Q. but there was a significant left hemisphere greater than right hemisphere difference in phase shift duration and I.Q. There also were significant frequency effects with the alpha frequency band exhibiting the lowest correlations and the theta and beta frequency bands exhibiting the strongest correlations between phase reset and intelligence. There also was a statistically significant posterior-to-anterior electrode direction affect between phase shift duration and full scale I.Q. but not between I.Q. and phase locking. In reference to the hypotheses formulated in the introduction, all four null hypotheses are rejected by the findings in this study.

Non-age adjusted and age adjusted analyses exhibited statistically significant correlations between phase shift and lock durations. The high statistical sensitivity of PR as an estimate of the Wechsler full scale I.Q., is likely due to the fact that I.Q. tests are age normalized and, therefore, age is not a significant factor in the ability of phase reset to correlate with a standard I.Q. test even though phase shift and locking durations change dramatically as a function of age (Thatcher et al., in press).

Limitations of this study

One limitation of the present study is the use of a linked ear reference which may reduce the ability to identify hemispheric differences, especially differences in temporal lobes. However, we do not consider the use of a linked ear reference as a limitation of phase reset itself based on the studies of Rappelsberger (1989), Kamiński and Blinowska (1991) and Essl and Rappelsberger (1998) concluded that linked ears were a valid and useful reference in the measurement of coherence although digital averaging of the ears is an optimal reference. Most importantly, the issue of a linked ear reference is irrelevant because none of the correlations with intelligence observed in this study can be explained by a reference effect since the same reference was used for all of the subjects. Another limitation of the study is the lack of a higher density array of electrodes with a higher spatial sampling. Improved spatial resolution should aid in identifying more localized phase reset processes. The lack of a 3-dimensional source analysis is another limitation since information about how local brain regions shift and lock phase is important. However, it is necessary to measure the surface EEG phase reset properties first, such as in this paper, in order to interpret 3-dimensional source phase reset. We plan to evaluate the correlations between intelligence and LORETA phase reset in a future study. Finally, because of space limitations we were unable to present and contrast the correlations of the various sub-tests of the Wechsler I.Q. test and such analyses are ongoing.

Table 4

Summary of correlations between full scale I.Q. and phase shift duration using a limited electrode set to test anterior-to-posterior and posterior-to-anterior directions, distance (6 cm, 12 cm, 18 cm and 24 cm) and hemisphere

Frequency	Left		Right	
	A-P	P-A	A-P	P-A
6 cm				
delta	0.326	0.521	0.249	0.852*
theta	0.792*	0.067	−0.015	0.418
alpha	0.734	0.876**	0.589	0.954****
beta1	0.823*	0.868**	0.648	0.793*
beta2	0.209	0.874**	0.117	0.858**
beta3	−0.471	0.594	0.696	0.823*
hi-beta	0.112	0.781*	0.268	0.600
12 cm				
delta	0.494	0.794*	0.619	0.794*
theta	−0.469	−0.050	−0.838*	−0.241
alpha	0.150	0.524	0.196	0.859**
beta1	−0.043	0.529	0.147	0.262
beta2	−0.319	−0.673	−0.258	0.630
beta3	−0.453	−0.619	0.318	−0.256
hi-beta	0.200	0.666	0.309	−0.661
18 cm				
delta	0.294	−0.059	0.199	0.664
theta	−0.747	−0.543	−0.698	0.447
alpha	−0.023	0.290	0.222	0.942***
beta1	0.330	0.183	−0.626	0.531
beta2	−0.696	−0.300	−0.660	−0.070
beta3	−0.112	−0.685	0.620	−0.809**
hi-beta	−0.262	0.309	0.408	0.023
24 cm				
delta	0.014	0.014	−0.194	−0.194
theta	−0.648	−0.648	−0.504	−0.504
alpha	0.130	0.130	0.626	0.626
beta1	0.598	0.598	0.147	0.147
beta2	−0.277	−0.277	−0.106	−0.106
beta3	−0.612	−0.612	−0.503	−0.503
hi-beta	−0.715	−0.715	−0.055	−0.055

Correlations between full scale IQ and phase shift duration.
Asterisks * signify the level of statistical significance.
Significant at *P*: * .05 ** .01 *** .001 **** .0001.

Table 5

Summary of correlations between full scale I.Q. and phase lock duration using a limited electrode set to test anterior-to-posterior and posterior-to-anterior directions, distance (6 cm, 12 cm, 18 cm and 24 cm) and hemisphere

Frequency	Left		Right	
	A-P	P-A	A-P	P-A
6 cm				
delta	−0.172	−0.875**	0.189	−0.669
theta	−0.616	−0.930***	−0.489	−0.895**
alpha	−0.704	0.108	−0.533	0.433
beta1	−0.638	−0.788*	−0.764*	−0.796*
beta2	−0.797*	−0.800*	−0.363	−0.699
beta3	−0.985****	−0.828*	−0.610	−0.748
hi-beta	−0.110	−0.376	−0.440	−0.700
12 cm				
delta	−0.083	−0.766*	0.083	−0.564
theta	−0.619	−0.610	−0.661	−0.315
alpha	−0.345	0.771*	0.198	0.865**
beta1	−0.191	−0.632	0.026	−0.372
beta2	−0.527	−0.677	0.005	−0.647
beta3	−0.438	−0.443	0.133	−0.873**
hi-beta	−0.289	−0.679	−0.282	−0.101
18 cm				
delta	−0.239	−0.063	0.032	0.083
theta	−0.622	−0.704	−0.368	−0.542
alpha	0.184	0.079	0.185	0.290
beta1	0.111	0.234	0.700	0.343
beta2	−0.143	−0.666	−0.366	−0.663
beta3	0.057	−0.556	−0.674	0.082
hi-beta	0.149	−0.294	−0.392	−0.014
24 cm				
delta	0.278	0.278	0.562	0.562
theta	−0.624	−0.624	−0.529	−0.529
alpha	0.177	0.177	0.173	0.173
beta1	0.142	0.142	0.634	0.634
beta2	−0.778*	−0.778*	−0.389	−0.389
beta3	−0.405	−0.405	−0.343	−0.343
hi-beta	0.148	0.148	0.036	0.036

Correlations between full scale IQ and phase lock duration.
Asterisks * signify the level of statistical significance.
Significant at *P*: * .05 ** .01 *** .001 **** .0001.

A two compartmental model of phase shift and phase lock

Pyramidal cells typically do not oscillate in isolation, however, they do have resonant properties that are modeled by the time constants of currents flowing through ionic channels (Hu et al., 2002; Steriade et al., 1990; Crook et al., 1998; Galan et al., 2005). Nonlinear oscillations in cortical networks are generated by a balance between relatively “slow” or long duration excitatory postsynaptic potentials (EPSPs) arising on the dentrites of neurons that are connected in cortico-cortical loops and local “short” duration

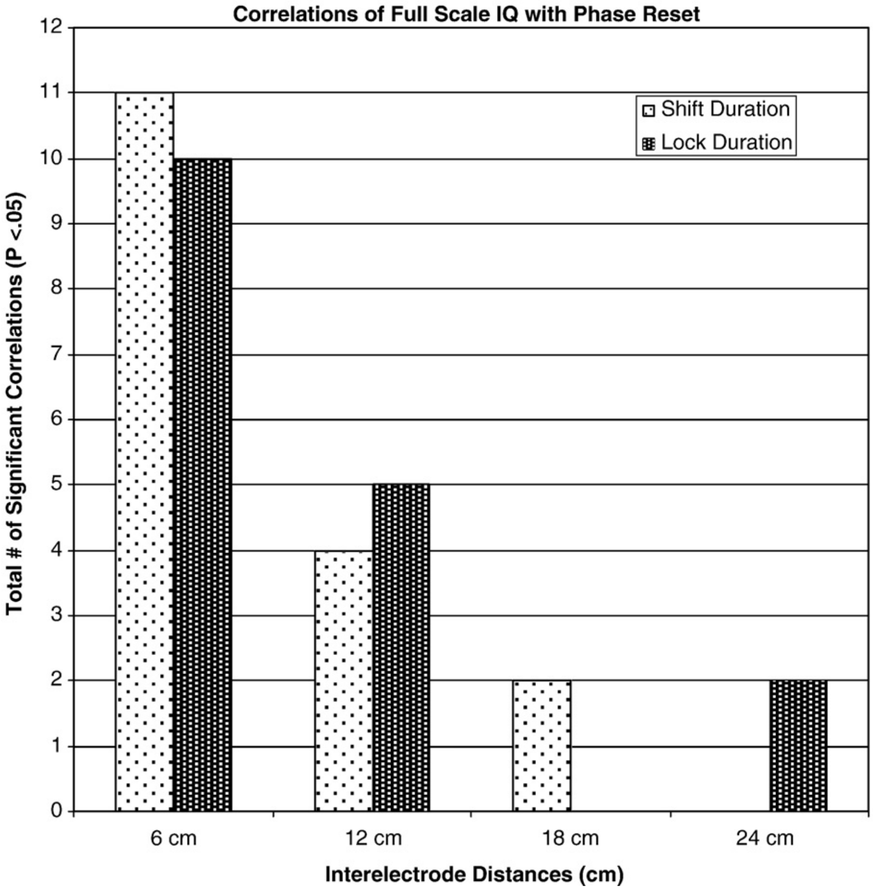

Fig. 7. Summary of the total number of statistically significant correlations between full scale I.Q. and phase shift duration and phase lock duration. The short interelectrode distances (6 cm) were the most significant.

inhibitory postsynaptic potentials (IPSPs) arising near the cell bodies of the pyramidal cells. Recurrent and lateral inhibition are involved in the selection of local neural circuits and the coupling between neural loops (Steriade et al., 1990; Buzsaki, 2006). Many studies have shown that the duration of bursts of inhibitory postsynaptic potentials (IPSPs) alters the firing pattern of neurons and determines the frequency of the EEG (Mainen and Sejnowski, 1995; 1996; Thomson, 2000a; 2000b; Buzsaki, 2006). The shorter the duration of the IPSP then the higher the mean frequency of the EEG. Thus, the primary candidate for phase shift duration in the present study is the action of inhibitory interneurons that shift the frequency of coupled nonlinear oscillators. An important property of nonlinear oscillators is that they exhibit a domain of entrainment in which the faster oscillating members entrain slower oscillating members within a limited frequency difference called the “synchronization region” and/or “Arnold Tongue” (Pikovsky et al., 2003). Thus, it is hypothesized that phase shift duration reflects the process of local neural assembly selection by the action of inhibitory interneurons that shift the frequency of coupled nonlinear oscillators. Phase locking, on the other hand, represents the sustained excitation in coupled loops of neurons that have been selected by the action of the frequency shifting inhibitory neurons. The question remains, however, what determines the phase shift and is there a reference phase to which the shift is based on? Buzsaki (2002, 2006) and Dragoi and Buzsaki (2006) and others (Fries et al., 2001; O'Keefe and Recce, 1993; Raghavachari et al., 2001, 2006; Lee et al, 2005; Tiesinga et al., 2008) have shown that the timing of action potentials is related to the phase of the hippocampus and entorhinal theta rhythms and that, in fact, neurons encode or store the phase relationship to the local field potentials (LFP) surrounding the neurons. It would be consistent with this literature to hypothesize that the phase shift in the present study is related to the encoding of phase information and phase locking is related to sustaining the phase encoding for an extended period of time in sub-assemblies of neurons. Release from phase locking by a subsequent phase shift represents a recoding to a different phase relationship to the local rhythmic field potentials and thus, the LFP is a reference phase. Small clusters of neurons exhibit bursts of action potentials synchronized to a preferred phase of the theta rhythm (Buzsaki, 2002; 2006; Tiesinga et al., 2008). Thus, it is hypothesized that the greater the difference between the phase of the LFP and the preferred phase of a given neural assembly then the longer the phase shift duration. A two compartmental model is proposed with compartment one being the local field potential (LFP) and compartment two the neural assemblies embedded in and phase synchronized to the preferred phase of the LFP. That is,

$$\Delta\Theta = \Phi_{\mathrm{LFP}} - \Phi_{\mathrm{Pref}} \tag{11}$$

where $\Delta\Theta$ is the phase difference in degrees between the local field potential phase and the preferred phase of the LFP that a particular neural assembly is coupled to. The larger the $\Delta\Theta$ then the longer is the phase shift duration (SD) or

$$\mathrm{SD} \propto \Delta\Theta \tag{12}$$

and full scale I.Q. is proportional to the average phase shift between the LFP and the preferred phase of action potential firing in a given sub-assembly of neurons or

$$\mathrm{I.Q.} \propto \frac{1}{N}\sum_{i=0}^{N}\Delta\Phi. \tag{13}$$

Fig. 8 is an illustration of a Local Field Potential model of phase shift duration and intelligence. According to this model, higher I.Q. subjects recruit a larger number of neural assemblies with longer phase differences with respect to the LFP than lower I.Q. subjects.

Intelligence, resource allocation and phase reset

As explained in the Introduction, PR is comprised of a phase shift followed by phase locking and is considered to be an important mechanism in EEG synchronization and desynchronization. Phase shift duration is a period of high uncertainty and instability, whereas, phase locking is a period of stability and low uncertainty (Freeman et al., 2003; Thatcher et al., in press). Analyses of the development of phase shift duration and phase locking characterized the phase shift process in terms of the theory of "self-organized criticality" in which phase shift (i.e., 40–80 ms) approaches "chaos" followed by phase locking or "stability" (100 ms to approximately 800 ms) (Thatcher et al., in press). According to this model, the ratio of "chaos" to "stability" varies as a function of age and frequency band and the number and/or density of neurons available for phase locking.

As mentioned previously, phase shift is relative to the ongoing background rhythms of the local field potential (LFP) which reflect excitability cycles and involve encoding of phase information. The role of phase shift is to identify neural assemblies that are not refractory and are otherwise available for binding together locally and globally. Once the available resources are phase shifted and phase coded to the background EEG rhythm then the neural assemblies become phase locked as a collective to mediate a given function. When phase shift duration is too short then there are fewer neural resources available to be phase locked into a stable dynamic. Longer phase shift duration increases the probability of identifying larger numbers of neurons capable of being phase locked and this is why there is a direct relationship between shift duration and I.Q. When phase shift duration is too long then there is increased noise and reduced number of neurons available for phase locking. When phase lock duration is too long then there is less flexibility and there are reduced resources available to be allocated by the phase shift mechanism. However, too short of phase locking will result in less information processing and less efficiency of the allocated resources with premature release of the resources by a subsequent phase shift. In short, an optimal balance between phase shift duration and phase lock duration is related to higher levels of intelligence because of an optimal balance which results in maximum speed and efficiency of information processing.

Fig. 9 illustrates a two compartmental resource allocation hypothesis to explain the relationship between phase shift duration (SD) and phase lock duration (LD) and intelligence. Both phase shift and phase locking can be represented by an inverted 'U' shaped function with I.Q. on the *y*-axis and shift duration (Fig. 9, upper right) or lock duration (Fig. 9, lower right) on the *x*-axis. The inverted 'U' shaped function shows an optimal level of SD or LD as a function of I.Q. The parabolic curves in Fig. 9 are normalized by taking the square and then the square root so that the curves are folded into the half plane and then the SD and LD curves are combined to a single inverted 'U' shaped function by mapping to the unit circle and representing LD and SD by cos theta and −cos theta, respectively. Time is mapped on the *x*-axis in degrees, for SD the degrees range from 180° to 90° and for LD the degrees range from 0° to 90° and the two different processes are related by an optimization of I.Q. in the upper half of the unit circle so that:

$$\mathrm{SD} = (-\cos\Theta_{SD})_i + (A\sin\Theta_{\mathrm{SD}})_j \tag{14}$$

and

$$\mathrm{LD} = (A\cos\Theta_{\mathrm{LD}})_i + (A\sin\Theta_{\mathrm{LD}})_j \tag{15}$$

and

$$\mathrm{I.Q.} \propto k\frac{\hat{\mathrm{SD}}}{\hat{\mathrm{LD}}} \tag{16}$$

where k = proportionality constant, $\hat{\mathrm{SD}}$ = average time bounded phase shift duration and $\hat{\mathrm{LD}}$ = average time bounded phase lock duration and I.Q. is directly proportional to the average shift duration of assemblies of neurons and inversely proportional to the average lock duration of assemblies of neurons. The time boundaries are hypothesized to be directly related to the average duration of inhibitory post synaptic potentials (IPSPs) and excitatory post synaptic potentials (EPSPs) with respect to the phase of the local field potential (LFP). Local IPSPs produce a change in frequency and a phase shift and the time required to shift phase between the phase of the LFP and the preferred phase of synchrony is the phase shift duration or SD (see Eq. (11)). Intermediate and long distant excitatory post synaptic potentials (EPSPs) that arise on the dendrites of cortical pyramidal cells involve excitatory feedback loops and exhibit a longer duration than the IPSPs and the average EPSP duration and loop oscillations determine the phase lock duration that follows a phase shift. In summary, phase shift duration is positively related to the average local IPSP duration on cell bodies and the phase lock duration is positively related to the average EPSP summation on the dendrites of cortical pyramidal cells.

EEG frequency, intelligence and phase reset

The theta and beta frequency bands exhibited the highest correlations between phase shift duration and I.Q. (see Fig. 4). Alpha frequency bands exhibited relatively weak correlations between shift duration and I.Q. and the vast majority of the correlations between shift duration and I.Q. were positive, i.e., the longer the shift duration the higher the I.Q. In contrast, the theta frequency band exhibited the strongest correlations between phase lock duration and I.Q. with the beta 2 (15–18 Hz) band exhibiting the next strongest correlation. The vast majority of the correlations between lock duration and I.Q.

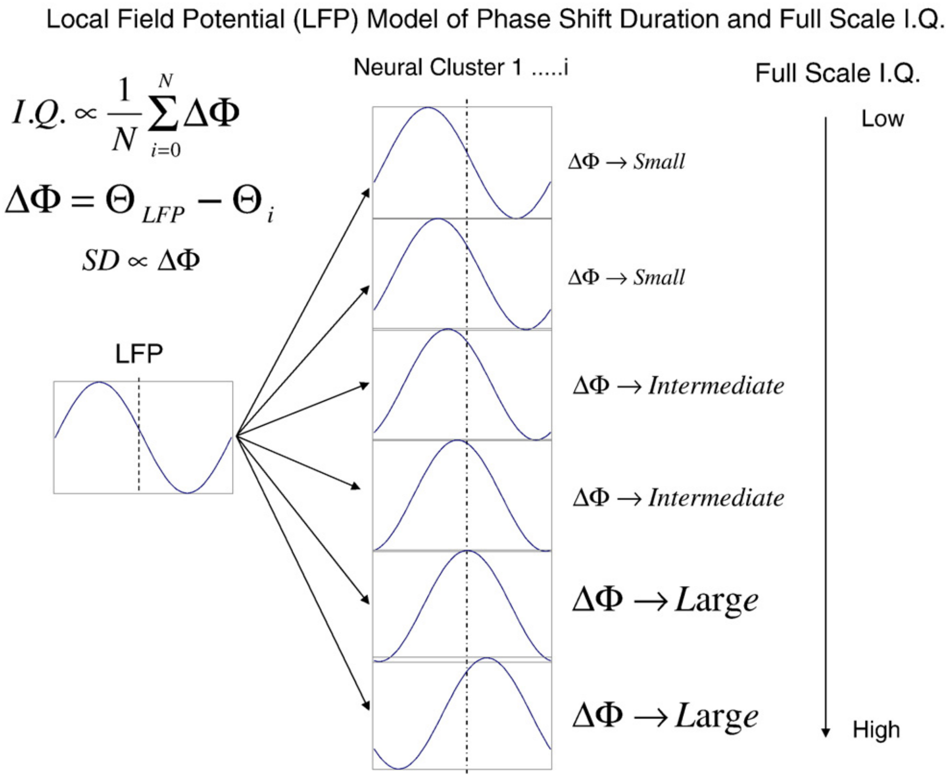

Fig. 8. Local Field Potential (LFP) model of phase shift duration (SD) and full scale I.Q. $\Delta\Phi$=difference in phase between the preferred phase of the LFP and the actual phase of the LFP. The greater the difference then the greater is SD and the higher is I.Q. Higher I.Q. subjects were able on the average to synchronize more neural assemblies with greater phase differences with respect to the phase of the LFP than lower I.Q. subjects.

were negative, i.e., the shorter the lock duration the higher the I.Q. It would appear that phase shift and phase lock are somewhat independent processes with phase locking more associated with the lower frequency bands and shift duration more related to the theta band as well as higher EEG frequencies. This is consistent with the fact that IPSPs are

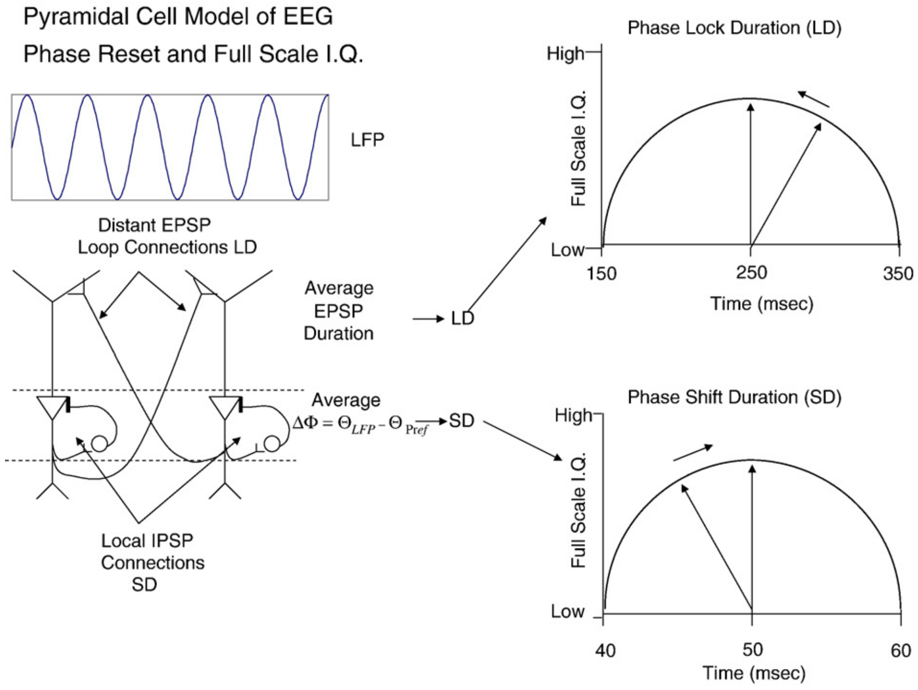

Fig. 9. Optimization model of intelligence and phase reset. Left top is the local field potential model (LFP) and lower right is an example of a neural assembly that exhibits a preferred phase relationship to the LFP. The right top is an inverted 'U' optimization curve expressing the relationship between full scale I.Q. and phase lock duration (LD) and the lower right is an optimization curve expressing the relationship between full scale I.Q. and phase shift duration (SD). Different time scales for LD and SD can be normalized by mapping to the unit circle as described in Eqs. (14) and (15).

much shorter in duration than are EPSPs and thus are involved in the higher frequencies of the EEG and this is consistent with the hypothesized role of inhibitory neurons in frequency shifting and nonlinear oscillator selection and recruitment as the phase shift process (Buzsaki, 2006). This indicates that neural resource identification and allocation is mediated by phase shifts primarily but not exclusively in the higher frequency bands and that phase locking occurs more in the delta and theta frequency band due to a wider spatial domain and thus a larger number of neurons that can be phase locked.

The findings indicate preferred frequencies, especially the theta and beta frequency bands, for phase encoding in which a phase shift is with respect to a particular phase of the background theta rhythm (LFP), similar to that hypothesized by Dragoi and Buzsaki (2006) for the hippocampal theta rhythm. The absence of a strong correlation in the alpha frequency band indicates that the frequency range from 8 to 13 Hz is not involved in phase coding per se but represents an “idling” state in which neural assemblies are available to quickly shift frequency to the theta and/or beta frequency bands in which local and global phase encoding occurs.

Increased event related desynchronization (ERD) is characterized by a reduction in EEG amplitude after the onset of a task and the theta frequency band is often associated with short-term memory processes (Klimesch et al., 2006, 2007). Although the present study recorded EEG on the same day as the I.Q. tests and not during a task, nonetheless, the findings suggest a linkage between ERD and phase locking by the fact that shorter lock durations are likely related to reduced average EEG amplitude. That is, less average theta phase locking is directly related to higher I.Q. and less average synchrony per unit time results in lower EEG amplitude.

Intelligence, hemispheric differences and posterior vs. anterior locations

There were statistically significant differences in the correlation of phase shift duration and intelligence with stronger correlations in the left hemisphere in comparison to the right. In contrast, there were no significant differences between left and right hemisphere in the correlations between phase lock duration and intelligence. This finding indicates that there are widespread spatial correlations between phase lock duration, independent of hemisphere. The results of the analysis also showed a significant direction affect in which there was a stronger correlation in posterior regions than in frontal regions for phase shift duration but there were no significant differences between frontal vs. posterior locations in the correlation of phase lock duration and intelligence. The finding of stronger correlations in posterior regions suggests that regions of higher packing density, such as in the posterior cortex, may be a relevant factor in the determination of the length of phase shift duration (Thatcher et al; in press). The findings also suggest that there are basic differences between phase shift and phase locking with phase locking less anatomically differentiated than phase shifting.

EEG coherence, intelligence and phase reset

Negative correlations between EEG coherence and I.Q. especially in the frontal lobes have been reported in several studies (Barry et al., 2002; Marosi et al., 1999; Martin-Loeches et al., 2001; Silberstein et al., 2003; Thatcher et al., 1983; 2005). Investigations by Thatcher et al. (2007a) demonstrated a direct relationship between coherence and phase lock duration and an inverse relationship to phase shift duration. The findings in the present study are consistent with previous studies of the relationship between intelligence and coherence and the relationship between phase reset and coherence. That is, increased I.Q. scores are correlated with shorter phase lock duration and longer phase shift duration both of which are correlated with lower coherence. This indicates that phase shift duration (SD) and phase lock duration (LD) are the elemental components of EEG coherence and these components represent dynamics involved in information processing. Measures of phase shift duration and phase lock duration are important in understanding the underlying dynamics of coherence itself and provide a micro-view of the inhibitory and excitatory control mechanisms involved in entrainment and neural assembly selection.

Acknowledgments

We are indebted to Drs. Rebecca McAlaster, David Cantor and Michael Lester and Ms. Sheila Ignasius and Ms. Diane Pruit for their involvement in the recruitment, EEG testing and evaluation of subjects and Rebecca Walker and Richard Curtin for database management. Informed consent was obtained from all subjects in this study. This research was supported by grants from USDA HRD-0200, USDA CSRS 801-12-09C and NIH Grant RR-08079-09).

References

Anokhin, A.P., Lutzenberger, W., Birbaumer, N., 1999. Spatiotemporal organization of brain dynamics and intelligence: an EEG study in adolescents. Int. J. Psychophysiol. 33 (3), 259–273.

Barry, R.J., Clarke, A.R., McCarthy, R., Selikowitz, M., 2002. EEG coherence in attention-deficit/hyperactivity disorder: a comparative study of two DSM-IV types. Clin. Neurophysiol. 113 (4), 579–585.

Bendat, J.S., Piersol, A.G., 1980. Engineering Applications of Correlation and Spectral Analysis. John Wiley and Sons, New York.

Bloomfield, P., 2000. Fourier Analysis of Time Series: an Introduction. John Wiley and Sons, New York.

Breakspear, M., Terry, J.R., 2002a. Detection and description of non-linear interdependence in normal multichannel human EEG data. Clin. Neurophysiol. 113 (5), 735–753.

Breakspear, M., Terry, J.R., 2002b. Nonlinear interdependence in neural systems: motivation, theory and relevance. Int. J. Neurosci. 112 (10), 1263–1284.

Breakspear, M., Williams, L.M., 2004. A novel method for the topographic analysis of neural activity reveals formation and dissolution of ‘dynamic cell assemblies’. J. Computational Neurosci. 16, 49–68.

Buzsaki, G., 2002. Theta oscillations in the hippocampus. Neuron 33, 325–340.

Buzsaki, G., 2006. Rhythms of the Brain. Oxford Univ. Press, New York.

Bruns, A., 2004. Fourier, Hilbert and wavelet-based signal analysis: are they really different approaches? J. Neurosci. Methods 137 (2), 321–332.

Chavez, M., Le Van Quyen, M., Navarro, V., Baulac, M., Martinerie, J., 2003. Spatio-temporal dynamics prior to neocortical seizures: amplitude versus phase couplings. IEEE Trans. Biomed. Eng. 50 (5), 571–583.

Cooper, R., Winter, A.L., Crow, H.J., Walter, W.G., 1965. Comparison of subcortical, cortical and scalp activity using chronically indwelling electrodes in man. Electroencpehalogr Clin Neurophysiol 18, 217–222.

Cosmelli, D., David, O., Lachaux, J.P., Martinerie, J., Garnero, L., Renault, B., Varela, F., 2004. Waves of consciousness: ongoing cortical patterns during binocular rivalry. Neuroimage 23 (1), 128–140.

Crook, S.M., Ermentrout, G.B., Bower, J.M., 1998. Dendritic and synaptic effects in systems of coupled cortical oscillators. J. Computation Neurosci. 5, 315–329.

Damasio, A.R., 1989. Time-locked multiregional retroactivation: a systems-level proposal for the neural substrates of recall and recognition. Cognition 33, 25–62.

Dragoi, G., Buzsaki, G., 2006. Temporal encoding of place sequences by hippocampal cell assemblies. Neuron 50, 145–157.

Essl, M., Rappelsberger, P., 1998. EEG coherence and reference signals: experimental results and mathematical explanations. Med. Biol. Eng. Comput. 36, 399–406.

Freeman, W.J., Rogers, L.J., 2002. Fine temporal resolution of analytic phase reveals episodic synchronization by state transitions in gamma EEGs. J. Neurophysiol 87 (2), 937–945.

Freeman, W.J., Burke, B.C., Homes, M.D., 2003. Aperiodic phase re-setting in scalp EEG of beta–gamma oscillations by state transitions at alpha–theta rates. Hum Brain Mapp 19 (4), 248–272.

Freeman, W.J., Homes, M.D., West, G.A., Vanhatlo, S., 2006. Fine spatiotemporal structure of phase in human intracranial EEG. Clin Neurophysiol 117 (6), 1228–1243.

Fries, P., Reynolds, J.H., Rorie, A.E., Desimone, R., 2001. Modulation of oscillatory neuronal synchronization by selective visual attention. Science 291, 1560–1563.

Galan, R.F., Ermentrout, G.B., Urban, N.N., 2005. Efficient estimation of phase-resetting curves in real neurons and its significance for neural-network modeling. Phys. Rev. Lett. 94 (15) 188–164.

Giannitrapani, D., 1985. The Electrophysiology of Intellectual Functions. Kargere, Press, New York.

Granger, C.W.J., Hatanka, M., 1964. Spectral Analysis of Economic Time Series. Princeton University Press, New Jersey.

Haier, R.J., Siegel, B., Tang, C., Abel, I., Buchbaum, M.S., 1992. Intelligence and changes in regional cerebral glucose metabolic rate following learning. Intelligence 16, 415–426.

Hu, H., Vervaeke, K., Storm, J.F., 2002. Two forms of electrical resonance at theta frequencies, generated by M-current, h-current and persistent Na$^+$ current in rat hippocampal pyramidal cells. J. Physiol (Lond) 545, 783–805.

John, E.R., 1968. Mechanisms of Memory. Academic Press, New York.

John, E.R., 2002. The neurophysics of consciousness. Brain Res. Brain Res. Rev 39 (1), 1–28.

John, E.R., 2005. From synchronous neural discharges to subjective awareness? Progress in Brain Research Vol. 150, 143–171.

Kahana, M.J., 2006. The cognitive correlates of human brain oscillations. J. Neurosci. 26, 1669–1672.

Kamiński, M., Blinowska, K.J., 1991. A new method of the description of the information flow in the brain structures. Biol.Cybern 65, 203–210.

Kirschfeld, K., 2005. The physical basis of alpha waves in the electroencephalogram and the origin of the “Berger effect”. Biol. Cybem. 92 (3), 177–185.

Klimesch, W., Doppelmayr, M., Hanslmayr, S., 2006. Upper alpha ERD and absolute power: their meaning for memory performance. Progress in Brian Res. 159, 151–165.

Klimesch, W., Sauseng, P., Hanslmayr, S., Gruber, W., Freunberger, R., 2007. Event-related phase reorganization may explain evoked neural dynamics. Neuroscience and Behavioral Rev. 31, 1003–1016.

Lachaux, J.-P., Rodriguez, E., Le Van Quyen, M., Lutz, A., Martinerie, J., Varela, F.J., 2000. Studying single-trials of phase synchronous activity in the brain. Int. J. Bifuc. Chaos. 10 (10), 2429–2439.

Lee, K.H., Williams, L.M., Breakspear, M., Gordon, E., 2002. Synchronous Gamma activity: a review and contribution to an integrative neuroscience model of schizophrenia. Brain Res. Rev. 41, 57–78.

Lee, H., Simpson, G.V., Logothetis, N.K., Rainer, G., 2005. Phase locking of single neuron activity to theta oscillations during working memory in monkey extrastriate visual cortex. Neuron 45, 147–156.

Le Van Quyen, M., Foucher, J., Lachaux, J.-P., Rodriguez, E., Lutz, A., Martinerie, J., Varela, F.J., 2001a. Comparison of Hilbert transform and wavelet methods for the analysis of neuronal synchrony. J. Neurosci. Methods 111 (2), 83–89.

Le Van Quyen, M., Martinerie, J., Navarro, V., Varela, F.J., 2001b. Characterizing neurodynamic changes before seizures. J. Clin. Neurophysiol. 18 (3), 191–208.

Lopes Da Silva, F.H., 1995. Dynamic of electrical activity of the brain, networks, and modulating systems. In: Nunez, P. (Ed.), Neocortical Dynamics and Human EEG Rhythms, pp. 249–271.

Lopes Da Silva, F.H., Pijn, J.P., 1995. Handbook of Brain Theory and Neural Networks. MIT Press, Arbib, Cambridge.

Mainen, Z.F., Sejnowski, T.J., 1995. Reliability of spike timing in neocortical neurons. Science 268, 1503–1506.

Mainen, Z.F., Sejnowski, T.J., 1996. Influence of dendritic structure on firing pattern in model neocortical neurons. Nature 382, 363–366.

Martin-Loeches, M., Munoz-Ruata, J., Martinez-Lebrusant, L., Gomez-Jari, G., 2001. Electrophysiology and intelligence: the electrophysiology of intellectual functions in intellectual disability. J. Intellect. Disabil. Res. 45 (1), 63–75.

Marosi, E., Rodriguez, H., Harmony, T., Yanez, G., Rodriquez, M., Bernal, J., Fernandez, T., Silva, J., Reyes, A., Guerrero, V., 1999. Broad band spectral parameters correlated with different I.Q. measurements. Int J Neurosci. 97 (1–2), 17–27.

McCartney, H., Johnson, A.D., Weil, Z.M., Givens, B., 2004. Theta reset produces optimal conditions for long-term potentiation. Hippocampus 14 (6), 684–697.

Netoff, T.I., Schiff, S.J., 2002. Decreased neuronal synchronization during experimental seizures. J. Neurosci. 22 (16), 7297–7307.

Nunez, P., 1995. Neocortical Dynamics and Human EEG Rhythms. Oxford University Press, New York.

O'Keefe, J., Recce, M.L., 1993. Phase relationship between hippocampal place units and the EEG theta rhythm. Hippocampus 3, 317–330.

Oppenheim, A.V., Schafer, R.W., 1975. Digital Signal Processing. Printice-Hall, London.

Otnes, R.K., Enochson, L., 1978. Applied Time Series Analysis. John Wiley and Sons, New York.

Pikovsky, A., Rosenblum, M., Kurths, J., 2003. Synchronization: a Universal Concept in Nonlinear Sciences. Cambridge Univ. Press, New York.

Press, W.H., Teukolsky, S.A., Vettering, W.T., Flannery, B.P., 1994. Numerical Recipes in C. Cambridge University Press, Cambridge, U.K.

Raghavachari, S., Kahana, M., Rizzuto, D.S., Caplan, J.B., Kirschen, M.P., Bouirgeois, B., Madsen, J.R., Lisman, J.E., 2001. Gating of human theta oscillations by a working memory task. J. Neuroscie. 21, 3175–3183.

Raghavachari, S., Lisman, J.E., Tully, M., Madsen, J.R., Bromfield, E.B., Kahana, M., 2006. Theta oscillations in human cortex during a working-memory task: evidence for local generators. J. Neurophysiol 95 (3), 1630–1638.

Rappelsberger, P., 1989. The reference problem and mapping of coherence: a simulation study. Brain Topog. 2 (1/2), 63–72.

Rizzuto, D.S., Madsen, J.R., Bromfield, E.B., Schultz-Bonhage, A., Seelig, D., Aschenbrenner-Scheibe, R., Kahana, M.J., 2003. Reset of human neocortical oscillations during a working memory task. Proc. Natl. Acad Sci. U S A. 100 (13), 7931–7936.

Roelfsmema, P.R., Engel, A.K., Konig, P., Singer, W., 1997. Visuomotor integration is associated with zero time-lag synchronization among cortical areas. Nature 385 (6612), 157–161.

Rudrauf, D., Douiri, A., Kovach, C., Lachaux, J.P., Cosmelli, D., Chavez, A., Renault, B., Marttinerie, J., Le Van Quyen, M., 2006. Frequency flows and the time-frequency dynamics of multivariate phase synchronization in brain signals. Neuroimage 31, 209–227.

Savitzky, A., Golay, M.J.E., 1964. Smoothing and differentiation of data by simplified least squares procedures. Analytic Chemistry 36, 1627–1639.

Silberstein, R.B., Song, J., Nunez, P.L., Park, W., 2004. Dynamic sculpting of brain functional connectivity is correlated with performance. Brain Topogr. 16 (4), 249–254.

Silberstein, R.B., Danieli, F., Nunez, P.L., 2003. Fronto-parietal evoked potential synchronization is increased during mental rotation. Neuroreport. 14 (1), 67–71.

Stam, C.J., van der Made, Y., Pijnenburg, Y.A.L., Scheltens, P.H., 2002a. EEG synchronization in mild cognitive impairment and Alzheimer's disease. Acta. Neurol. Scand. 106, 1–7.

Stam, C.J., van Cappellen vanWalsum, A.M., Pijnenburg, Y.A.L., Berendse, H.W., de Munck, J.C., Scheltens, P.H., van Dijk, B.W., 2002b. Generalized synchronization of MEG recordings in Alzheimer's disease: evidence for involvement of the gamma band. J. Clin. Neurophysiol. 19, 562–574.

Stam, C.J., de Bruin, E.A., 2004. Scale-free dynamics of global functional connectivity in the human brain. Hum. Brain Map. 22, 97–109.

Steriade, M., Gloor, P., Linas, R., Lopes da Silva, F.H., Mesulam, M.M., 1990. Basic mechanisms of cerebral rhythmic activity. EEG and Clin. Neurophysiol. 76, 481–508.

Tallon-Baudry, C., Bertrand, O., Fischer, C., 2001. Oscillatory synchrony between human extrastriate areas during visual short-term memory maintenance. J. Neurosci. 21 (20), RC177.

Tass, P.A., 1997. Phase Resetting in Medicine and Biology. Springer-Verlag, Berlin.

Tass, P.A., Rosenblum, M.G., Weule, J., Kurths, J., Pikovsky, A., Volkmann, J., aSchnitzler, A., Freund, H.J., 1998. Detection of n:m phase locking from nosy data: application to magnetoencephalography. Phys. Rev. Lett. 81 (15), 3291–3294.

Tesche, C.D., Karhu, J., 2000. Theta oscillations index human hippocampal activation during a working memory task. Proc. Natl. Acad Sci. U S A. 18 (97(2)), 919–924.

Thatcher, R.W., McAlaster, R., Lester, M.L., Horst, R.L., Cantor, D.S., 1983. Hemispheric EEG asymmetries related to cognitive functioning in children. In: Perecuman, A. (Ed.), Cognitive Processing in the Right Hemisphere. Academic Press, New York.

Thatcher, R.W., Krause, P., Hrybyk, M., 1986. Corticocortical association fibers and EEG coherence: a two compartmental model. Electroencephalog. Clinical Neurophysiol. 64, 123–143.

Thatcher, R.W., Walker, R.A., Guidice, S., 1987. Human cerebral hemispheres develop at different rates and ages. Science 236, 1110–1113.

Thatcher, R.W., Biver, C., McAlaster, R., Salazar, A.M., 1998. Biophysical linkage between MRI and EEG coherence in traumatic brain injury. NeuroImage 8 (4), 307–326.

Thatcher, R.W., Walker, R.A., Biver, C., North, D., Curtin, R., 2003. Quantitative EEG normative databases: validation and clinical correlation. J. Neurotherapy 7 (No.3/4), 87–122.

Thatcher, R.W., North, D., Biver, C., 2005. EEG and intelligence: univariate and multivariate comparisons between EEG coherence, EEG phase delay and power. Clinical Neurophysiology 116 (9), 2129–2141.

Thatcher, R.W., North, D., Biver, C.J., 2007a. Development of cortical connections as measured by EEG coherence and phase. Human Brain Mapping, Oct., early publication.

Thatcher, R.W., Biver, C.J., North, D., 2007b. LORETA current source correlations and intelligence. Human Brain Mapping 28 (2), 118–133.

Thatcher, R.W., Biver, C.J., North, D., in press. Self-organized criticality and the development of EEG phase reset. Human Brain Mapping. (Jan. 24, Electronic publication ahead of print).

Thomson, A.M., 2000a. Facilitation, augmentation and potentiation at central synapses. Trends Neurosci. 23, 305–312.

Thomson, A.M., 2000b. Molecular frequency filters at central synapses. Prog. Neurobiol. 62, 159–196.

Tiesinga, P., Fellows, J.M., Sejnowski, T.J., 2008. Regulation of spike timing in visual cortex. Nature Reviews 9 (2), 97–109.

Tononi, G., Sporns, O., Edelman, G.M., 1994. A complexity measure for selective matching of signals by the brain. Proc. Natl. Acad. Sci. USA 93, 3422–3427.

Vaadia, E., Haalman, L., Abeles, M., Bergman, H., Prut, Y., Slovin, H., Aertsen, A., 1995. Dynamics of neuronal interactions in monkey cortex in relation to behavior events. Nature 373 (6514), 515–518.

Varela, F.J., 1995. Resonant cell assemblies: a new approach to cognitive functions and neuronal synchrony. Biol. Res. 28 (1), 81–95.

Varela, F.J., Lachaux, J.-P., Rodriguez, E., Martinerie, J., 2001. The brainweb: phase synchronization and large-scale integration. Nat. Rev., Neurosci. 2 (4), 229–239.

Watts, D.J., Strogatz, S.H., 1998. Collective dynamics of “small-world” networks. Nature 393, 440–442.